Electrochimica Acta 122 (2014) 39–49

Contents lists available at ScienceDirect

Electrochimica Acta

journal homepage: www.elsevier.com/locate/electacta

Spectroelectrochemical studies of poly(N-methylaniline) formation, redox behaviour and degradation. A comparison with polyaniline

G.A. Planes [a], J.L. Rodriguez [b], M.C. Miras [a], E. Pastor [b], C.A. Barbero [a,*]

[a] Dpto de Química, Universidad Nacional de Río Cuarto, 5800, Río Cuarto, Argentina
[b] Dpto. de Química Física, Universidad de la Laguna, 38071, Tenerife, España

ARTICLE INFO

Article history:
Received 28 June 2013
Received in revised form 23 October 2013
Accepted 24 October 2013
Available online 7 November 2013

Keywords:
In-situ infrared spectroscopy
Mass spectroscopy
Poly(*N*-methylaniline)
Oxidation

ABSTRACT

Spectroelectrochemical methods, in-situ Fourier Transform Infrared (FTIR) and Differential Electrochemical Mass Spectroscopy (DEMS), are used to study the formation of poly(*N*-methylaniline) (PNMANI) by anodic oxidation of *N*-methylaniline (NMANI). The methods are used to elucidate the structural changes during redox switching of PNMANI and the nature of the degradation products of PNMANI produced during electrochemical oxidation. The results are discussed in comparison with those previously reported for aniline. The early stages of NMANI oxidation leads to the formation of dimers by head-to-tail coupling (product = *N,N′*-dimethyl-4-aminodiphenylamine, DMADA) and tail-to-tail coupling (product = *N,N′*-dimethylbenzidine, DMBz). It seems that, when *N*-methylaniline is oxidized, it is formed more tail-to-tail dimer than in the case of aniline, due to steric and electronic effects of the N-substituent methyl groups. The head-to-tail dimer (DAMADA) is irreversibly adsorbed on the electrode surface. The elucidation of the reaction mechanism is aided by electrochemical and in-situ spectroelectrochemical studies of *N,N′*-dimethylaniline which can only give the tail-to-tail dimer (*N,N,N′,N′*-tetramethylbenzidine, TMB). The in-situ FTIR study of redox behaviour of poly(*N*-methylaniline) shows that quinonimine units are produced during oxidation. The intensity of the band at 1196 cm^{-1}, assigned to C-N^+ stretching in the -C-N^+-CH_3 moiety, increases due to an increased substituted imine content in the oxidized film. An increase of the anion (perchlorate) concentration inside the film, due to compensation of the positive charges formed during oxidation, is also detected by FTIR. CO_2 formation is observed by FTIR during NMANI oxidation and in electrochemically induced polymer degradation. The formation of CO_2 is confirmed by DEMS. Additionally, during degradation, indophenol like molecules together with quinone, are produced as the final organic degradation product

1. Introduction

The oxidation of aromatic amines was extensively studied in the past using voltammetric techniques combined with chemical synthesis of products. [1,2] The interest in the field has been renewed owing to the role of those compounds as monomers of conducting polymers. [3] It is assumed that electropolymerization of aromatic amines begins with amine oxidation to radical cation. The radical cation undergoes fast follow up chemical reactions. Using mainly comparison of the cyclic voltammetric response for amine oxidation and those of the chemically synthesized dimers, Bacon & Adams,[4] found that dimers, head-to tail (N-C4) (4-aminodiphenylamine, 4ADA) and tail-to-tail (C4-C4′) (benzidine, Bz), are the products of aniline oxidation.

In the oxidation of *N*-methylaniline (NMANI), Galus and Adams,[5] found that the main product is dimethylbenzidine (DMBz) and another product due to the reaction of DMBz with two molecules of NMANI. They did not detect the product of head-to-tail coupling. The simple comparison of voltammetric responses has limited value in reaction mechanism elucidation. In-situ spectroscopic techniques, such as differential electrochemical mass spectroscopy (DEMS) [6] and in-situ FTIR [7],originally used to study the electrochemical behavior of simple organic compounds [8,9], have been afterward applied to study more complex compounds. [10–12] Schmiemann et al. investigated the adsorption and electrochemical reactions of aniline using DEMS. [13] Nakayama et al. investigated polyaniline formation by time resolved FTIR under potentiostatic control. [14] Cases et al. studied aniline,[15] and diphenylamine oxidation [16] at pH 5. Holze [17] analyzed the adsorption and oxidation of aniline using SERS. Dunsch and coworkers used ATR, [18] and EPR [19,20] combined with UV-vis to investigate aniline oxidation. In contrast to that, in-situ FTIR has been used extensively to study the redox processes in polyaniline,

* Corresponding author.
E-mail address: cbarbero@exa.unrc.edu.ar (C.A. Barbero).

0013-4686/$ – see front matter © 2013 Elsevier Ltd. All rights reserved.
http://dx.doi.org/10.1016/j.electacta.2013.10.179

mainly by internal reflection (ATR) [21–26] and less by external reflection [27–29]. In situ Raman spectroscopy (including SERS and Resonant Raman) has also been extensively used to investigate polyaniline. [30–35]

The presence of a substituent at the nitrogen atom in *N*-methylaniline should have a significant effect on the properties of the polymer. Indeed, the redox coupled ion exchange,[36] and the effect of anions on the cyclic voltammogram [37] are considerably different to those of polyaniline. Several studies have been published on poly(*N*-methylaniline) preparation and properties [38–41]. It has been shown, based in magnetic and chemical studies, that the partially oxidized polymer exists mainly in the dication form more than polarons associated with the emeraldine form of polyaniline [42]. Kilmartin and Wright studied the photoelectrochemical properties along with the Raman and XPS spectra of alkyl substituted polyanilines. [43]

Malinauskas and coworkers used UV-vis and Raman spectroelectrochemistry to study the polymerization initial stages of aniline [44], *N*-methylaniline [45,46] and others substituted anilines [47].Stassen and Hambitzer studied the oxidation of aniline and *N*-methylaniline using electrochemical thermospray mass spectrometry [48]. Contrary to the expected from previous work, they did not find benzidine as product of aniline oxidation. Only head-to tail dimers and trimers were observed. They also found that a head-to-tail product is formed during oxidation of *N*-methylaniline, together with the tail-to-tail product, which, according to that proposed by Galus and Adams, was the only product. As Adams et al. [49] early pointed out, both dimers, the head-to-tail and tail-to-tail could initiate polymerization and therefore will be included in the polymer structure, affecting the polymer properties. Therefore it is important to know which products are produced in the early stages of polymerization. Moreover, contamination of the polymer with benzidine should be avoided owing to its well known carcinogenicity. [50] Its retention inside the polymer, or production by polymer degradation, has been a concern when practical applications of the polymer are envisaged. [51] Furthermore, it has been reported that the presence of aniline dimers affects the polymerization rate and polymer morphology. [52–55] Therefore it is relevant to know which soluble species are present during polymer growth since they can affect the polymer morphology and aggregation.

Another valuable information, which could be obtained using in-situ techniques, involves the nature of the degradation products of poly(*N*-methylaniline). A final product, due to nucleophilic attack of water on the oxidized polymer, should be quinone,[56] but, unlike polyaniline, other species could be produced due to the presence of the alkylamine group.

In a previous work,[57] in-situ FTIR and DEMS were used to study the oxidation of aniline, the nature of soluble and adsorbed intermediates and the products of polyaniline degradation. It was shown that those techniques give valuable insight on the early stages of polymerization, the redox properties of the polymer and the electrochemically induced degradation. Here, the study is extended to the oxidation of *N*-methylaniline and the properties of the resulting polymer: poly(*N*-methylaniline). As poly(*N*-methylaniline) has been less thoroughly studied than polyaniline, there is an ongoing interest on this polymer in the materials chemistry field. [58–66]

2. Experimental

N-methylaniline (Fluka, analytical grade) was used as received. All others chemicals are of analytical grade. Solutions were prepared with ultrapure (Millipore) water and degassed by bubbling pure Ar. The electrochemical experiments were controlled by a computerized potentiostat (Heka).

Poly(*N*-methylaniline) was synthesized by cycling the electrode from 0.1 to 0.95 V vs. SHE at 50 mV s^{-1}. Three cycles to a more extreme potential (1.05 V vs. SHE) are used to initiate the polymerization.

2.1. Differential electrochemical mass spectroscopy (DEMS)

The working electrode (electrochemical area ca. 5.5 cm^2), consists of a Pt sputtered on a microporous semipermeable membrane (Scimat, average thickness 60 μm, porosity 50%, mean pore size 0.17 μm). The electrochemical cell was completed with a Pt wire as counter electrode and a standard hydrogen electrode (SHE) in the same acid electrolyte which is used as reference electrode. All potentials in the text are referred to this electrode. The DEMS cell is directly attached to the vacuum chamber containing the mass spectrometer (Balzers QMG 112) with a Faraday cup detector. Volatile species generated at the electrode evaporate at the pores of the membrane into the vacuum and are detected by the mass spectrometer with a time constant of ca. 1 s. This time constant is small enough to allow mass spectrometric cyclic voltammograms (MSCVs) for selected mass-to-charge ratios (*m/z*) to be recorded in parallel to cyclic voltammograms (CVs) at a scan rate of 0.01 V s^{-1}.

2.2. FTIR spectroelectrochemistry

The FTIR spectrometer was a Bruker Vector 22 provided with a mercury-cadmium telluride detector. Parallel (*p*) polarized IR light was employed unless otherwise specified. A glass cell with a 60°CaF_2 prism at its bottom was used. The cell and experimental arrangements were described previously. [67] Spectra were computed from the average of 128 scans obtained with resolution of 8 cm^{-1}. The reflectance ratio R/R_0 was calculated where R and R_0 are the reflectance of the electrode measured at the sampling and reference potential, respectively. In this way bands pointing upward (positive bands) are related to species which are present in a greater amount at the reference potential, whereas bands pointing downward (negative bands) correspond to species in a greater amount at the sample potential.

The working electrode was a Pt disk placed on one of the prism faces connected with a Pt wire. The disk was cleaned before each experiment by heating in a gas flame and washed with pure water.

3. Results and Discussion

3.1. N-methylaniline oxidation

The cyclic voltammogram of a 10 mM solution of *N*-methylaniline (NMANI (I)) in acid (0.1 M $HClO_4$) media is shown in Fig. 1.a. The voltammogram shows an oxidation peak (a) at ca. 1.15 V which is assigned to the oxidation of unprotonated amine. [68] In aqueous acid media most of NMANI is protonated but a fast equilibrium provides the unprotonated amine active in the electrochemical reaction. The oxidation peak (a) does not have a complementary reduction peak. This is likely to be due to the fact that electrochemical oxidation is coupled to fast dimerization reactions (Scheme 1). [69] Additionally, in successive cycles the current of peak (a) decreases more than expected by diffusion layer depletion and the peak potential shifts to more positive values. Moreover, new peaks systems (b-b′, c-c′ and d-d′) are present in the backward part of the first scan and successive cycles. The current decrease and peak potential shift of peak (a) are likely to be due to surface blocking by adsorbed products (dimers, oligomers, polymer). It has been shown that, even in the case of formation of

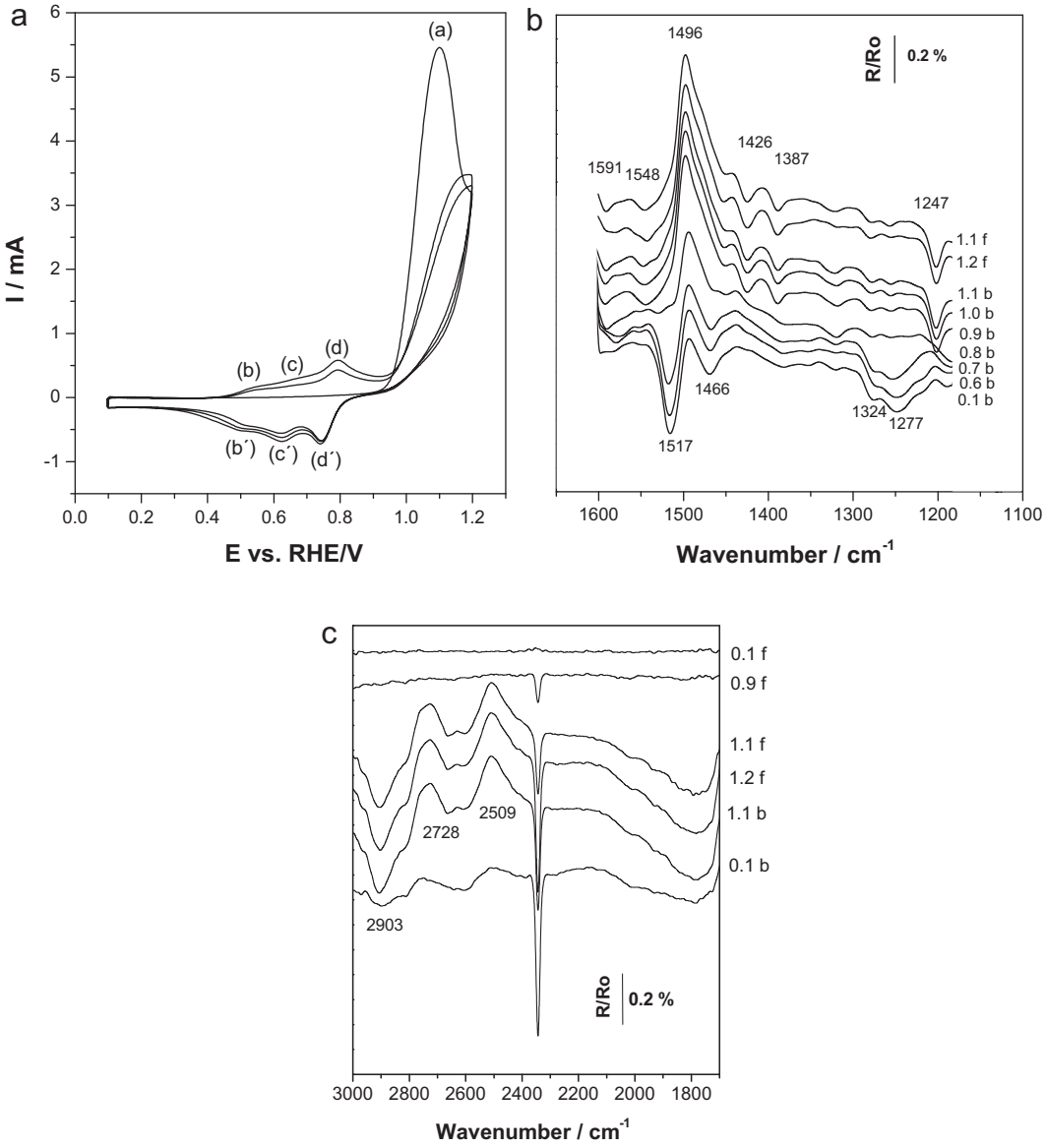

Fig. 1. (a) Cyclic voltammogram of N-methylaniline (10 mM/0.1 M $HClO_4$) on polycrystalline Pt at 50 mV s^{-1}. (b) In-situ FTIR measurements taken during oxidation of N-methylaniline (10 mM/0.1 M $HClO_4$) on polycrystalline Pt. p-polarized light. Region: 1600-1100 cm^{-1}. (c) In-situ FTIR measurements taken during oxidation of N-methylaniline (10 mM/0.1 M $HClO_4$) on polycrystalline Pt. p-polarized light. Region: 3000-1700 cm^{-1}.

electroactive polymers, the surface becomes less active towards soluble monomer oxidation. [70]

The dimerization reaction likely occurs by attack of the cation radical on a non oxidized amine molecule (Scheme 1). However, since the medium is highly polar, dimerization of two cation radical molecules can not be ruled out. [71] The electrophilic attack of the cation radical could be by the nitrogen towards the para position of the aromatic ring (head to tail, N-C4), giving N,N'-dimethyl-4-aminodiphenylamine (DMADA). Alternatively, the positive charge on the nitrogen delocalize in the aromatic ring and couples (tail to tail, C4-C4′) with a free amine molecule to give *N,N'*-dimethylbenzidine (DMBz). (Scheme 1). Although the reaction at the ortho position to the amine group is also possible, the corresponding dimer has not been detected. It is likely that steric factor precludes attack in the ortho position.

In analogy with aniline oxidation,[57] the peak system b-b′ is assigned to the oxidation/reduction of the dimer head-to-tail (DMADA) while the peak system d-d′ is due to the redox reactions of soluble dimer tail-to-tail (DMBz). DMBz oxidation occurs at a more anodic potential than DMADA due to the steric constraints of the biphenyl system in DMBz to transform into planar quinonimine by oxidation.

Another peak system (c-c′) is observed whose nature will be discussed below. The results are similar to those observed during aniline oxidation, but the peak system (d-d′) assigned to the tail-to-tail dimer shows a larger current intensity in the case of NMANI than in the case of aniline. It is likely that steric and inductive effect of the alkyl groups favor the formation of tail-to-tail over the head-to-tail coupling during NMANI oxidation. [72]

The FTIR spectra, taken during oxidation of *N*-methylanililine in acid media, are shown in Fig. 1.b and 1.c. In the region below 1600 cm^{-1} (Fig. 1.b), a positive band is observed at ca. 1496 cm^{-1}, which, in analogy to aniline oxidation, could be assigned to the aromatic stretching both in NMANI and DMBz. The negative bands (related to increased concentration of the absorbing species) are related to vibrations in the products: head-to-tail (N,N'-dimethyl-4-aminodiphenylamine, DMADA, (VII)) and tail-to-tail dimer (N,N′-dimethylbenzidine, DMBz, (IV)).

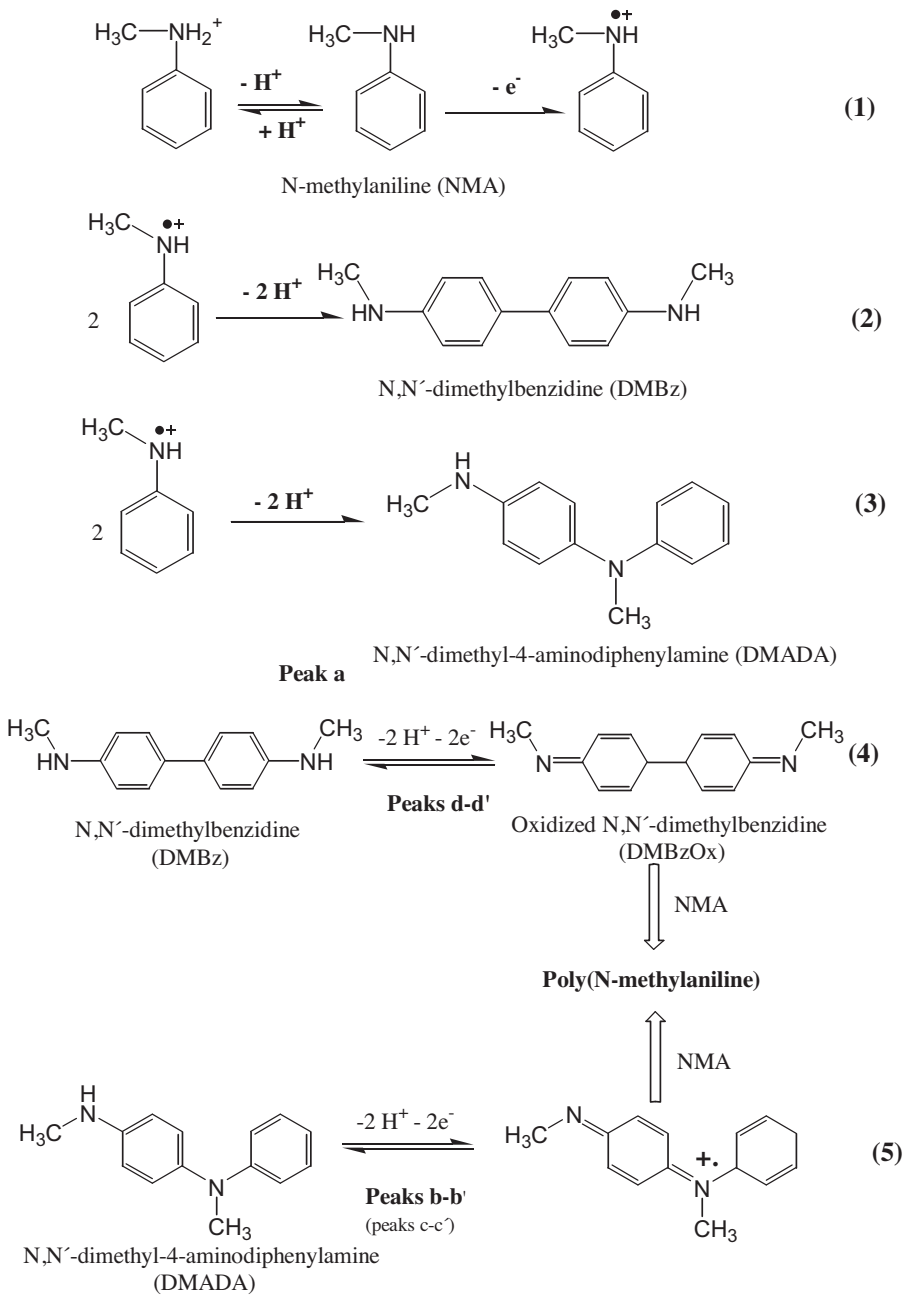

Scheme 1. Proposed mechanism of N-methylaniline electrochemical oxidation and chemical dimerization, followed by electrochemical reduction of dimers.

The negative bands (at 1591, 1548, 1426, 1387 and 1247 cm^{-1}) decrease in intensity when the potential is stepped below 0.9 V. Therefore, these bands are assigned to vibrations of oxidized products, which disappear on reduction. On the other hand, the negative bands at 1517, 1466, 1324 and 1277 cm^{-1}, which are not present at oxidation potentials, increase in intensity when the potential is stepped below 0.9 V. Therefore, these bands are assigned to vibrations of the reduced products. The band at 1517 cm^{-1} could be assigned to the aromatic stretching in DMADA. The band at 1591 cm^{-1} could be assigned to the stretching in the imine group (CH_3-N = C-). Indeed it is also observed in the FTIR spectra of the polymer and of tetramethylbenzidine (see below). The bands at 1426, 1277 and 1247 cm^{-1} could be assigned to bands in DMBz because they are also present in the difference spectrum of tetramethylbenzidine (see below). On the other hand the bands at 1548, 1466, 1387 and 1324 cm^{-1} seem to be related to vibrations of the oxidized DMADA as they decrease in intensity at potentials less positive than 0.6 V vs. SHE, when the dimer is reduced. (see Fig. 1.a). The negative band at 1582 cm^{-1} could be assigned to the C = N stretching in oxidized DMADA while the band at 1308 cm^{-1} is linked to the stretching of C-N^+-CH_3, present in the oxidized DMADA. The band at 1346 cm^{-1} is attributed to the bending of the–CH_3 group in oxidized DMBz, which frequency could be altered by mesomeric effect going from NMANI to oxidized DMBz. [73]

The bands at 1466 and 1247 cm^{-1}, which remain in the reduced products, are assigned to the degradation product: quinone in its reduced form (see degradation below). The spectra show also broad bands in the region above 2500 cm^{-1} (Fig. 1.c) which were not observed during the oxidation of aniline.[52] In this region, the bands at 2728 and 2509 cm^{-1} could be assigned to the N-H stretching of secondary amines. Upon oxidation of NMANI, the N-H disappears because the oxidized dimers formed do not contain N-H

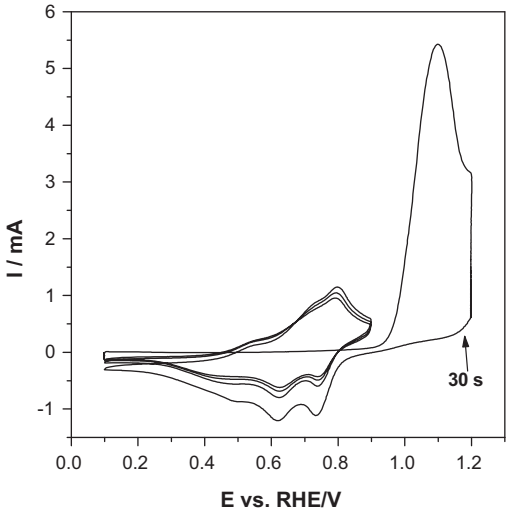

Fig. 2. Cyclic voltammogram of N-methylaniline to test the reaction between the oxidation product and N-methylaniline.

(Scheme 1). This concentration change is observed as an increase in the positive intensity (concentration at the measurement potential lower than at the reference) of the bands at 2728 and 2509 cm^{-1}. Upon reduction, most of the bands decrease to its original intensity due to formation of the reduced dimers which contain the same groups. The band at 2903 cm^{-1} is attributed to the N-H stretching of the charged (oxidized) dimer. This assignment agrees with the fact that the band of negative intensity increases upon oxidation and decreases upon reduction. It is noteworthy that the head-to-tail dimer (DMADA) remains charged (Scheme 1), compared with aniline which oxidized head-to-tail dimer (4-aminodiphenylamine, 4ADA) is not charged.[52] Such difference could explain why clear bands are observed in the high wavenumber region for NMANI, but they are not detected during aniline oxidation. Additionally, a clear band due to CO_2 formation (Fig. 1.c) is observed at 2340 cm^{-1}, which was not observed during oxidation of aniline. The band does not decreases during reduction. It is known that C-H bond can be broken by electrochemical oxidation on a Pt electrode. Therefore, some of the methyl groups,[74] present in NMANI can be oxidized to CO_2, during polymerization.

In the discussion above, the new bands have been assigned to reaction products. However, the new bands can be due to adsorbed reactant species whose vibration is shifted due to adsorption. To ascertain if this is the case, the spectra were also taken with s-polarized light (Fig. 2). It is well known that p-polarized light is more sensitive to surface species, due to orientation of the radiation dipoles at the metal/electrolyte interface. [75] Most bands show a similar behavior in the spectra obtained with s-polarized light (Supl. Info., Figure S1) precluding assignment to bands shifted by adsorption. The bands assignments are summarized in Scheme 2.

It was proposed,[13] that DMBz was the only product of NMANI oxidation and it reacts with free NMANI to give a product with electrochemical response shown by peak system b-b' in Fig. 1.a. To test such mechanism, a significant amount of the oxidation products were synthesized by waiting 30 s at 1.2 V vs. SHE. After that, the potential was cycled with and extreme positive potential enough to oxidize DMADA and DMBz but not enough positive to oxidize NMANI. As it can be seen (Fig. 2), there is not growth of the intensity of b-b' peaks, suggesting that these peaks do not correspond to the product of DMBz and NMANI but to DMADA. Also, the in-situ FTIR spectra (supl. information), taken with a similar potential program (albeit with potential steps), do not reveal formation of new products.

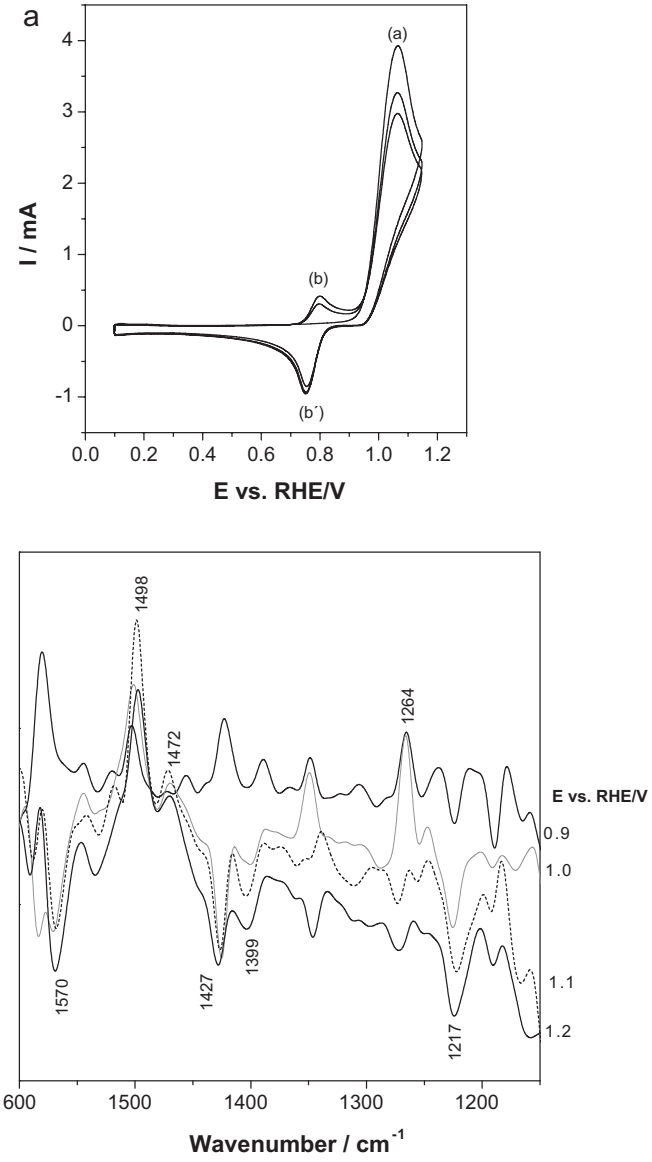

Fig. 3. Cyclic voltammogram of N,N′-Dimethylaniline (10 mM/0.1 M $HClO_4$) at 50 mV s^{-1}. In-situ FTIR measurements taken during oxidation of N,N′-Dimethylaniline (10 mM/0.1 M $HClO_4$).

An easy test of the mechanism could be made by measuring the CV and in-situ FTIR during oxidation of the related compound, N,N'-dimethylaniline (DMA). Since the amine has two alkyl groups at the nitrogen, it could not give the head-to-tail dimer (or the linear polymer) because the electrophilic substitution of the radical cation on the aromatic ring will form a charged quaternary ammonium group or promote the loss of a methyl cation. Any of these processes is more difficult than tail-to-tail coupling which involves only the loss of protons. Therefore the only product should be the tail-to-tail dimer (N,N,N',N'-tetramethylbenzidine, TMB) as shown in Scheme 3.

Indeed, the cyclic voltammogram (Fig. 3.a) shows a clear oxidation peak (a) which has not the corresponding reduction peak, indicating a fast coupled chemical reaction. However, the peak potential in the successive cycles remains the same and the peak current decreases slightly upon cycling, likely due to the depletion of the diffusion layer, unlike the CV of NMANI oxidation (Fig. 1.a). Therefore, there is no evidence of surface blocking in agreement with the fact that DMA does not polymerize easily. The product of

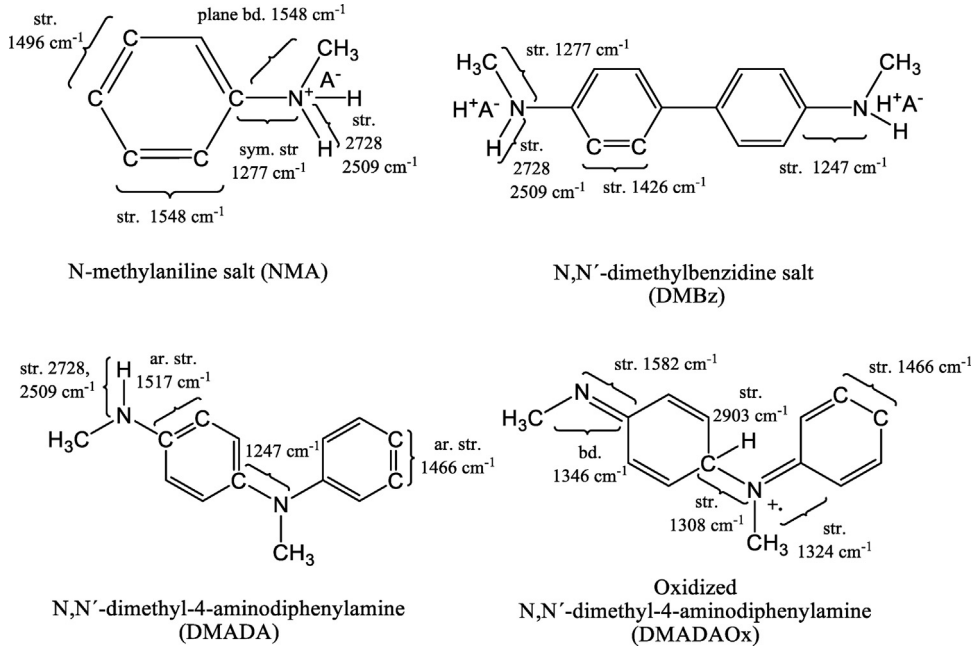

Scheme 2. Vibrational band assignment for NMANI dimeric species. The assignments are made by comparison with data from literature. A- are the anions present in the electrolyte (ClO_4^- in this work).

the chemical reaction shows a quasireversible peak couple (b,b') which has been attributed to TMB. [76] The FTIR spectra (Fig. 3.b) show bands due to TMB which help to assign the equivalent bands in *N*-methylaniline spectra.

3.2. Head to tail dimer (DMADA) adsorption

It has been usually assumed that only soluble intermediates are produced prior to anilines polymerization. On the other hand, it has been found by cyclic voltammetry,[77] that the head-to-tail dimer of aniline is irreversibly adsorbed onto the platinum electrode, giving a surface redox couple on the electrode. The adsorption was corroborated using in situ FTIR.[57] To test if that is also the case with DMADA, we used a flow cell. This allows exchange the polymerization solution with another free of monomer without losing the potential control. First, the potential was stepped to 1.2 V vs. SHE and kept for 2 min. Then the potential was set at 0.1 V vs. SHE and the cell content was exchanged 10 times by monomer free electrolyte, to assure removal of soluble species, without losing potential control.

The CV taken after that procedure (Fig. 4.a) shows clearly a quasireversible peak system due to an adsorbed redox couple. The peak positions match these of the peaks c-c′ in Fig. 1.a, suggesting that the peaks are due to the redox reaction of adsorbed DMADA produced during NMANI electrochemical oxidation. The FTIR difference spectrum of the oxidized dimer, taken at 0.8 V vs. SHE with 0.6 V vs. SHE as reference, (Fig. 4.b) shows a positive band at 1508 cm^{-1} and negative bands at 1582, 1378 and 1162 cm^{-1}. The band at 1508 cm^{-1} could be assigned to the aromatic stretching in DMADA while the band at 1582 cm^{-1} could be assigned to the stretching in the imine group (CH_3-N=C). The band at 1162 cm^{-1} could be assigned to the perchlorate ions, which are exchanged

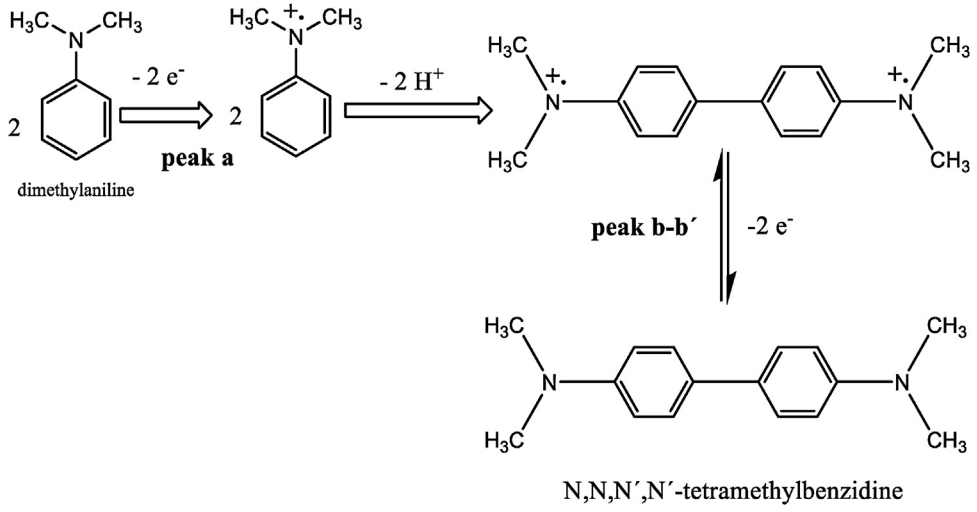

Scheme 3. Mechanism of N,N′-dimethylaniline electrochemical oxidation and dimerization.

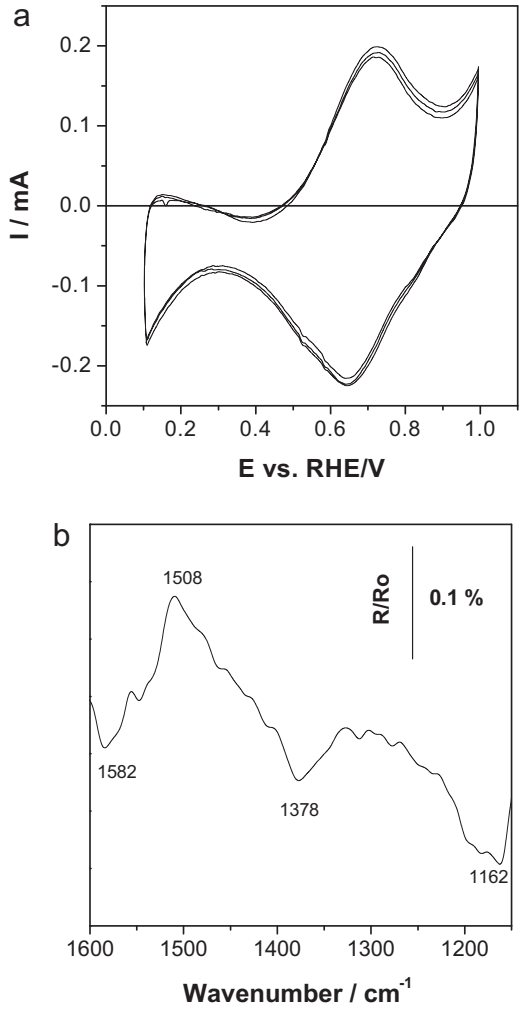

Fig. 4. Cyclic voltammogram of the adsorbate produced during oxidation of NMANI (10 mM) in 0.1 M $HClO_4$. The voltammogram is taken in monomer free solution (0.1 M $HClO_4$) at 50 mV s^{-1}. In-situ FTIR measurements taken during oxidation of the adsorbed dimer (0.1 M $HClO_4$) on polycrystalline Pt. p-polarized light, taken at 0.8 V vs. SHE with 0.6 V vs. SHE as reference.

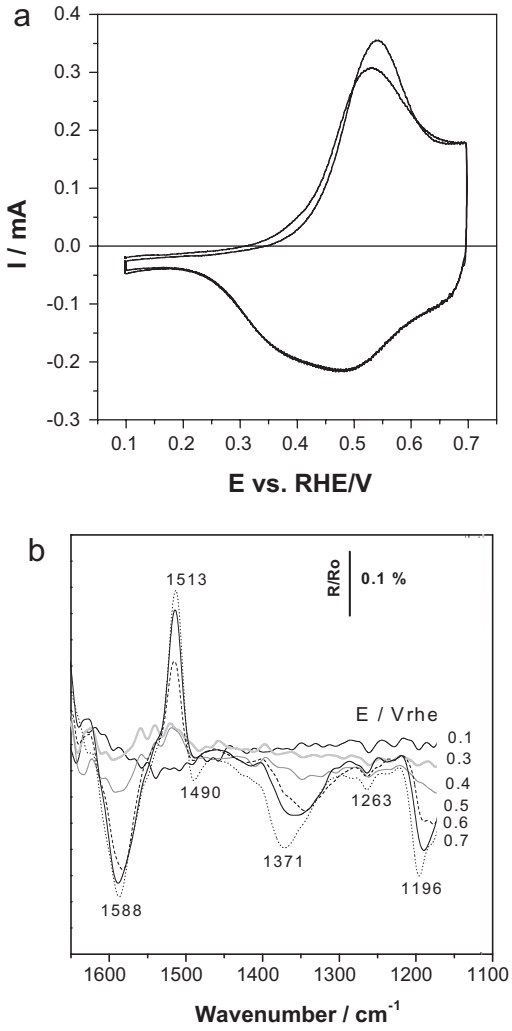

Fig. 5. Cyclic voltammogram of the polymer obtained by oxidation of poly(N-methylaniline)/Pt in 1 M $HClO_4$. In-situ FTIR measurements taken during oxidation/reduction of poly(N-methylaniline)/Pt in 1 M $HClO_4$.

during the oxidation-reduction of DMADA (left side reaction in Scheme 1. 1.As in the case of aniline,[57] the tail-to-tail dimer (DMBz) species seems not adsorb on the platinum surface.

3.3. Poly(N-methylaniline) redox switching

In situ FTIR is not only able to study soluble species but also indicate the structural changes occurring during the oxidation/reduction of the electroactive polymer produced by oxidation of NMANI. A thin polymer film of poly(*N*-methylaniline) was produced and its redox response was studied using cyclic voltammetry and in-situ FTIR. The cyclic voltammogram (first oxidation process) of a poly(*N*-methylaniline) film on Pt is shown in Fig. 5.a.

The redox peaks correspond to the first process described in Scheme 4. 4.Anion insertion should take place to compensate the positive charge formed inside the polymer. However, it is known that the reduced state could be partially protonated at pH 1. Therefore, the formation of positive charges inside the films is compensated by proton expulsion, released by the protonated part of the reduced state, and by anion insertion, in the non protonated part of the reduced state of the polymer. Such effects has been previously studied using Probe Beam Deflection and Electrochemical Quartz Microbalance.[37] Since such equilibria does not affect the structural changes during oxidation, for sake of simplicity, the leucomeraldine state of PNMANI is depicted unprotonated in Scheme 4.

The in-situ FTIR spectra show bands changing intensity when the oxidation state of the polymer is modified (Fig. 5.b). The intensity of the band at 1513 cm^{-1}, associated with C = C stretching of the amine aromatic rings, decreases upon oxidation due to the conversion of amine aromatic rings to quinonimine ring, during the change of leucomeraldine to emeraldine state (Scheme 4). Accordingly, the band at 1588 cm^{-1}, assigned to C = N and C = C stretching in the quinonimine units, increases intensity upon oxidation due to the formation of quinonimine units in the emeraldine state. The bands at 1490, 1371, and 1263 cm^{-1}, assigned to vibrations of the emeraldine state of PMANI (Scheme 5), show the same changes. The intensity of the band at 1196 cm^{-1}, assigned to C-N^+ stretching in the -C-N^+-CH_3 moiety, also increases because the relative concentration of the substituted imine augment in the oxidized film. This band could also be related to the Cl-O stretching in the counter anion (ClO_4^-). However, since the measurement is made trough a thin layer of electrolyte, the assignment is less clear in this case. The bands assignments are summarized in Scheme 5.

The spectra do not show clear bands above 1600 cm^{-1}. However, a broad absorption which is usually assigned to the

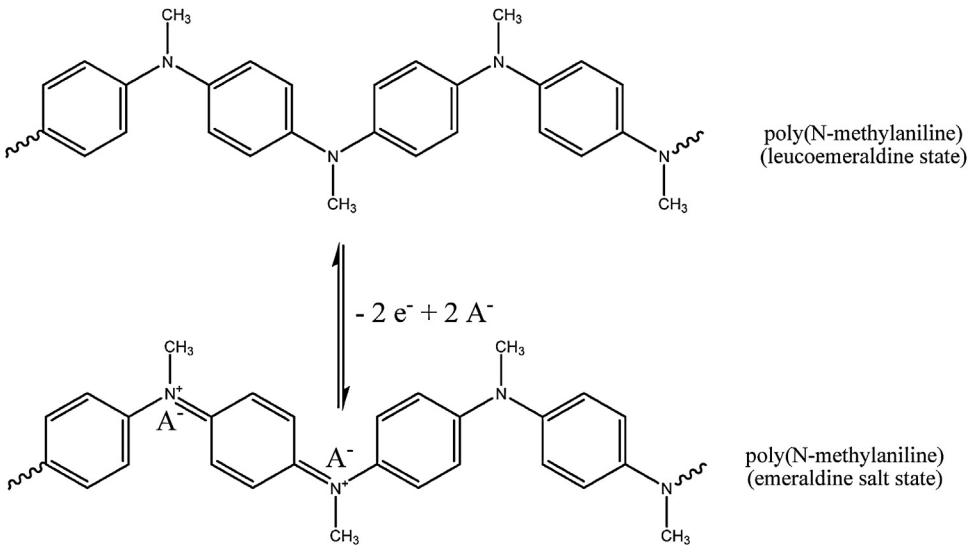

Scheme 4.

electronic transition to the conduction band of the polymer,[78] is detected at anodic potentials, where PNMANI is in its conductive state.

Unlike the case of polyaniline,[57] the cyclic voltammogram and in-situ FTIR spectra of poly(*N*-methylaniline) (Supl. Info, Figure S2) synthesized at lower monomer concentration (0.05 M/0.1 M $HClO_4$) are very similar to those described in Fig. 5. It seems that the lower conductivity of poly(*N*-methylaniline),[79] induces less shifting of the spectrum baseline.

3.4. Poly(N-methylaniline) electrochemical degradation.

As in the case of polyaniline,[57], [80] subjecting the polymer to potentials more anodic than the ones required to convert emeraldine to pernigraniline (higher than 0.9 V vs. SHE here), in acid aqueous media, produce changes associated with degradation of the polymer backbone. At these potentials the film is converted into its fully oxidized form (pernigraniline charged state) which is highly reactive to nucleophilic attack (Scheme 6). [81]

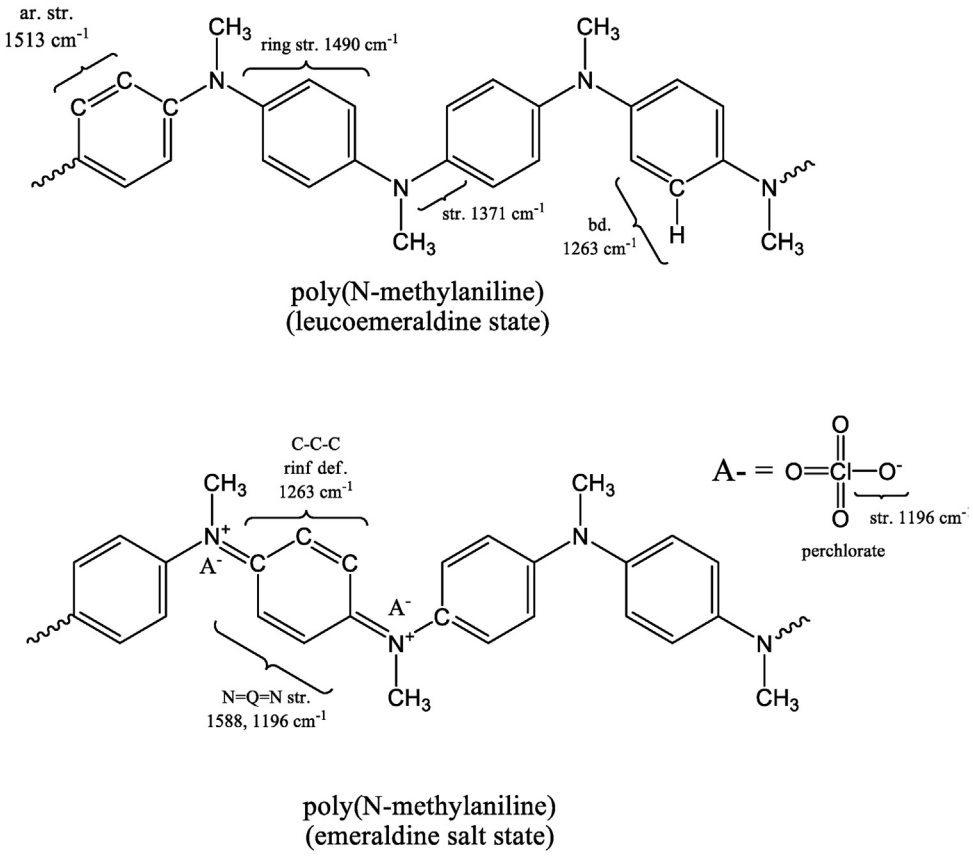

Scheme 5. Vibrational band assignment for poly(N-methylaniline) redox states. The assignments are made by comparison with data from literature.

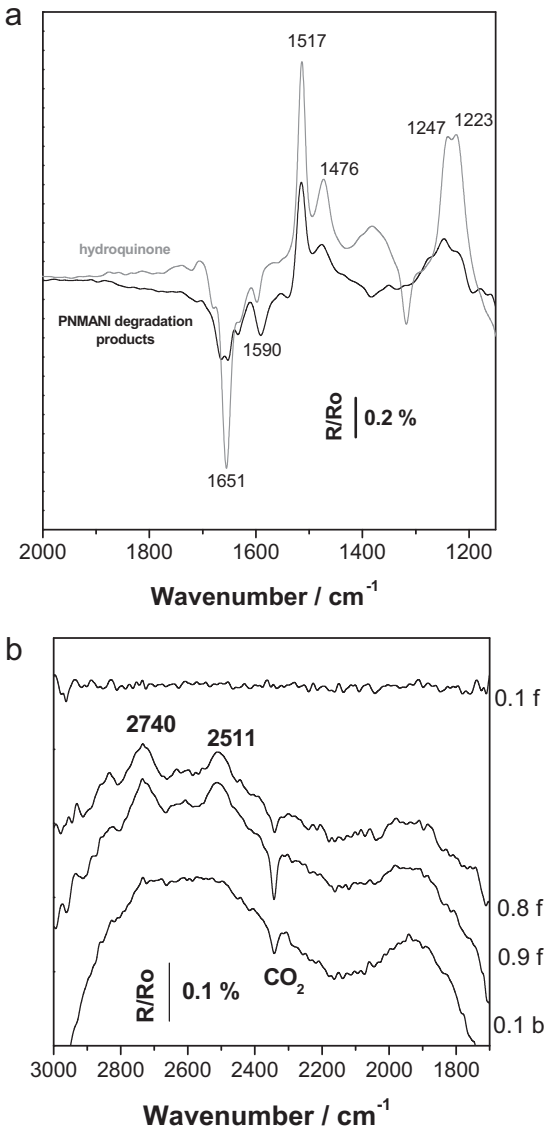

Fig. 6. In-situ FTIR difference spectrum (region between 1600 and 1200 cm^{-1}) of poly(N-methylaniline) degraded by oxidation at 1.2 V vs. SHE in 1 M $HClO_4$. The spectrum (black line) is taken at 0.8 V vs. SHE using the one taken at 0.1 V vs. SHE as reference. The spectrum of hydroquinone (10 mM/1 M $HClO_4$) measured in the same conditions is shown (grey line) for comparison. In-situ FTIR difference spectra (region between 3000 and 1800 cm^{-1}) of poly(N-methylaniline) degraded by oxidation at 1.2 V vs. SHE in 1 M $HClO_4$.

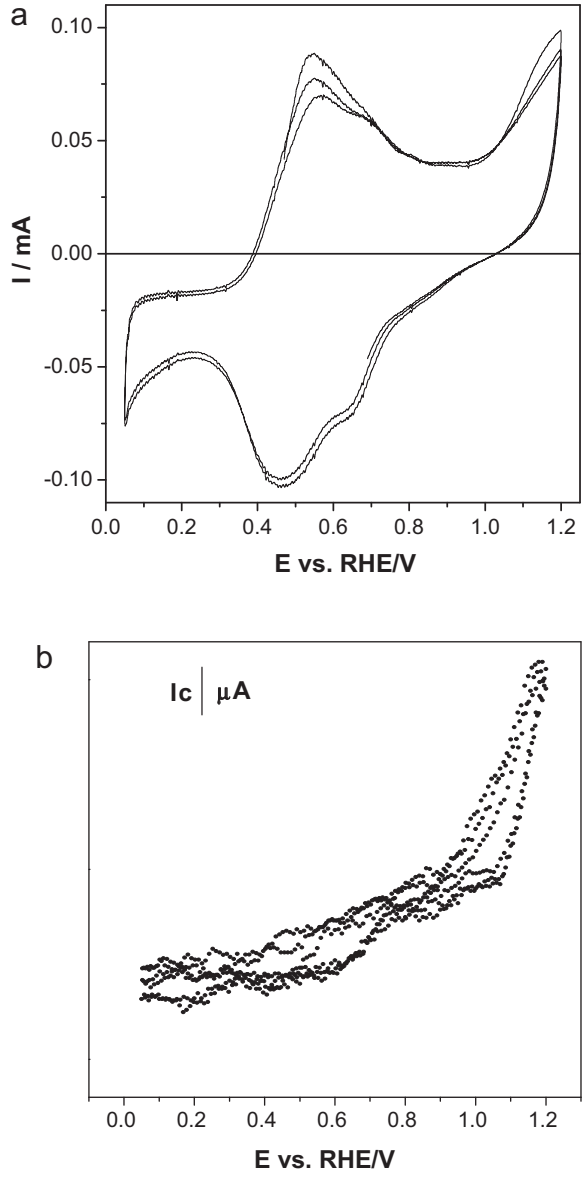

Fig. 7. CV (m/z = 44) during poly(N-methylaniline) degradation on a porous Pt electrodes. MSCV (m/z = 44) during poly(N-methylaniline) degradation on a porous Pt electrodes.

In monomer-free aqueous solution the best nucleophile is water which could attack the positive imine nitrogen giving rise to breaking the polymer chain (Scheme 6). The soluble products should be methylammonium ion and hydroquinone. Since the potentials are more positive than that of hydroquinone oxidation,[82] this species is converted to benzoquinone and could be reduced to hydroquinone by stepping to 0.1 V vs. SHE.

To find out the structure of the degradation products, poly(*N*-methylaniline) films were kept at a potential of 1.1 V vs. SHE, in 0.1 M $HClO_4$, for 400 s. The spectrum of the resulting solution was compared (at the same potential) with that of a solution of hydroquinone (Fig. 6.a). Most of the bands are present at the same wavenumber in both spectra, supporting the assignment of hydroquinone (converted to p-benzoquinone at the working potential) as the main degradation product. However, three bands appear at 2908, 2340 (negative), 2728 and 2509 cm^{-1} (positive). It is observed that the intensity of the band at 2340 cm^{-1} increases with oxidation and remains constant during reduction. This behaviour suggests that CO_2 is also produced during degradation of PNMANI films on Pt. DEMS data support such a conclusion (see below).

The bands at 2728 and 2509 cm^{-1}, previously assigned to–NH^+, increase in intensity during oxidation and decrease during reduction (Fig. 6.b). The same occurs with the one at 2908 cm^{-1}, assigned to–NH^+ charged dimer. This behaviour suggests that other species, like *N*-methylindofenol, are present in the solution after degradation. The bands at wavenumber above 2500 cm^{-1} are absent in the spectra taken during redox switching of PNMANI, at potentials below 0.8 V vs. SHE suggesting that vibrations of polymer groups are not related to the bands observed during degradation.

Successive scans up to 1.2 V vs. SHE show a broad peak at ca. 1.15 V vs. SHE, accompanied by decrease of the the peak current at ca. 0.5 V vs. SHE, where the redox response of the polymer is observed (Fig. 7.a). The monitoring species, using DEMS, of m/z= 44 during electrochemical cycling of PNMANI films up to 1.2 V vs. SHE (Fig. 7.b), reveals that a significant amount of CO_2 is produced at extreme anodic potentials. This result confirms that complete

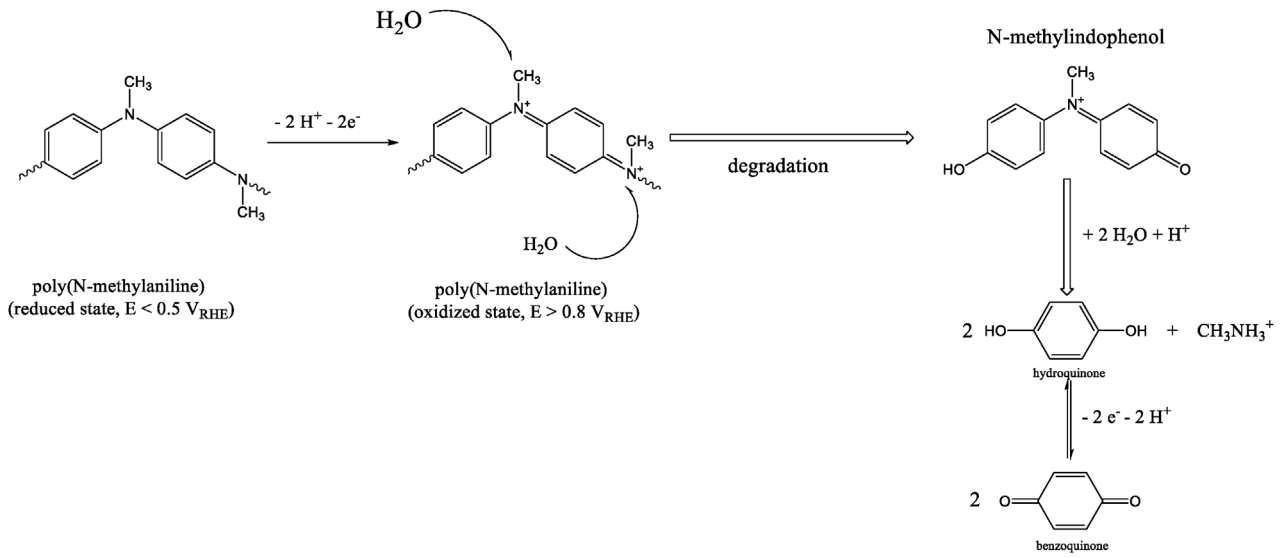

Scheme 6. Proposed mechanism of electrochemically induced degradation of poly(N-methylaniline).

oxidation of the polymer is possible on Pt electrodes. Indeed, by cycling between 0.1 and 1.5 V vs. SHE in monomer-free solution during more than 30 minutes, the film is completely removed from the Pt electrode. The same occurs with PANI. The electrode, after treatment, shows the voltammogram of a clean Pt surface and no CO_2 is detected by DEMS. The procedure is of interest to clean Pt electrodes covered with PANI or PNMANI films when other procedures (flame treatment, polishing, etc) can not be applied. Since polyanilines can be easily deposited on conductive substrates by electrochemical polymerization and could be removed by electrochemically induced degradation, they can be useful as masking material in the formation of micro or nanostructured surfaces. [83].

4. Conclusions

The early stages of *N*-methylaniline polymerization seem to be similar to those of aniline. The monomer is oxidized to its cation radical, which dimerizes. Two dimers are produced by head-to-tail (N,N′-dimethyl(4-aminodiphenylamine), DMADA) and tail-to-tail coupling (N,N′-dimethylbenzidine, DMBz). The FTIR study shows evidence of the formation of both dimers during *N*-methylaniline oxidation. However, it seems that more tail-to-tail dimer (DMBz) is formed when *N*-methylaniline is oxidized than in the case of aniline. This is likely to be due to steric and electronic effects of the methyl group on the head-to-tail coupling. Studying of a model compound (*N,N′*-dimethylaniline) allows to clearly identify the bands due to the tail-to-tail dimer (DMBz).

The head-to-tail dimer (DMADA) is adsorbed in the electrode surface, as shown by cyclic voltammetry and in-situ FTIR of the isolated adsorbed products by solution exchange under potential control.

The redox switching of poly(*N*-methylaniline) involves oxidation of amine units to quinonimine units, the oxidized units bear the charge which results in a shift of the vibrational bands. The intensity of the band assigned to C-N^+ stretching in the -C-N^+-CH_3 moiety, also increases due to a increased substituted imine content in the oxidized film. An increase of the anion (perchlorate) concentration inside the film, due to compensation of the positive charges formed during oxidation, is detected by FTIR.

During degradation of PNMANI, benzoquinone and protonated methylamine are produced by nucleophilic attack of water on the fully oxidized polymer. However, during both formation and degradation of PNMANI, other bands assigned to indophenol like compounds are also observed. Additionally, CO_2 is detected by in-situ FTIR and DEMS during formation and degradation of PNMANI. This means that the monomer and the polymer could be electrochemically burned on the Pt surface. Such process could be used to clean completely the electrode surface. However, it also means that extreme care should be taken with the potentials applied to Pt electrodes covered by poly(N-methylaniline) films, to avoid degradation of the polymer at the electrode/polymer interface to avoid partial disconnection of the polymer film from the electrode.

The fact that N-methylaniline and aniline oxidation show a similar reaction mechanism, suggests that the electrochemical oxidation and polymerization of different anilines should obey a general reaction mechanism such as the one described in Scheme 1.

Acknowledgements

C.A. Barbero and G.A. Planes are permanent research fellows of CONICET. The work was financed by MINECO (Spain) Project CTQ2011-28913-C02-02, SECYT-UNRC, CONICET, FONCYT and MinCyT-Cordoba (Argentina).

Appendix A. Supplementary data

Supplementary data associated with this article can be found, in the online version, at http://dx.doi.org/10.1016/j.electacta.2013.10.179.

References

[1] R.N. Adams, Electrochemistry at solid electrodes, Marcel Dekker, New York, 1969.
[2] H. Yang, A.-J. Bard, J. Electroanal. Chem., 339(1992)423-449 and references therein.
[3] H.S. Nalwa (Ed.), Handbook of Organic Conductive Molecules and Polymers, Conductive Polymers: Spectroscopy and Physical Properties, John Wiley & Sons, New York, 1997; A. Malinausakas, Synth. Met., 107(1999)75-83.
[4] J. Bacon, R.N. Adams, J. Amer. Chem. Soc. 90 (1968) 6596.
[5] Z. Galus, R.N. Adams, J. Phys. Chem 67 (1963) 862.
[6] A. Wieckowski, Interfacial Electrochemistry: Theory, Experiment, and Applications, Marcel Dekker, Inc. (1999) NY–USA.
[7] T. Iwasita, F.C. Nart, Advances in Electrochemical Science and Engineering, in: H. Gerischer, C.W. Tobias (Eds.), VCH, Weinheim, 1995.
[8] D. Kolbe, W. Vielstich, Electrochimica Acta 41 (1996) 2457–2460.
[9] R. Ianniello, V.M. Schmidt, U. Stimming, J. Stumper, A. Wallau, Electrochim. Acta 39 (1994) 1863–1869.
[10] V.M. Schmidt, J. Stumper, E. Pastor, J. Schmidberger, A. Hamelin, Surf. Science 335 (1995) 197–203.

[11] (a) J.L. Rodriguez, E. Pastor, X.H. Xia, T. Iwasita, Langmuir 16 (2000) 5479–5486; (b) E. Mendez, J.L. Rodriguez, M.C. Arevalo, E. Pastor, Langmuir 18 (2002) 763–772.
[12] J. Silva-Chong, E. Méndez, J.L. Rodríguez, M.C. Arévalo, E. Pastor, Electrochimica Acta 47 (2002) 15–19.
[13] U. Schmiemann, Z. Jusys, H. Baltruschat, Electrochimica Acta 39 (1994) 561–576.
[14] M. Nakayama, S. Saeki, K. Ogura, Analytical Sciences 15 (1999) 259–263.
[15] F. Cases, F. Huerta, P. Garcés, E. Morallón, J.L. Vázquez, J. Electroanal. Chem. 501 (2001) 186–192.
[16] F. Cases, F. Huerta, R. Lapuente, C. Quijada, E. Morallón, J.L. Vázquez, J. Electroanal. Chem. 529 (2002) 59–65.
[17] R. Holze, J. Electroanal. Chem. 250 (1988) 145–157.
[18] A. Zimmermann, U. Künzelmann, L. Dunsch, Synthetic Metals 93 (1998) 17–25.
[19] P. Rapta, R. Fáber, L. Dunsch, A. Neudeck, O. Nuyken, Spectrochimica Acta Part A 56 (2000) 357–362.
[20] A. Petr, L. Dunsch, J. Electroanal. Chem. 419 (1996) 55–59.
[21] Z. Ping, G.E. Nauer, H. Neugebauer, J. Theiner, J. Electroanal. Chem. 420 (1997) 301–306.
[22] Z. Ping, G.E. Nauer, H. Neugebauer, J. Theiner, A. Neckel, Electrochim. Acta 42 (1997) 1693–1700.
[23] Z. Ping, H. Neugebauer, A. Neckel, Electrochim. Acta 41 (1996) 767–772.
[24] Z. Ping, H. Neugebauer, A. Neckel, Synthetic Metals 69 (1995) 161–162.
[25] H. Neugebauer, A. Sariciftci, N.S. Neckel, H. Kuzmany, Synthetic Metals 29 (1989) 185–192.
[26] N.S. Sariciftci, M. Bartonek, H. Neugebauer, H. Kuzmany, A. Neckel, Synthetic Metals 29 (1989) 193–202.
[27] V.W. Jones, M. Kalaji, G. Walker, C. Barbero, R. Kötz, J. Chem. Soc. Farad. Trans 90 (1994) 2061–2066.
[28] K. Ogura, K. Nakaoka, M. Nakayama, J. of Electroanalytical Chemistry (2000) 119–125.
[29] M. Nakayama, M. Iino, K. Ogura, Journal of Electroanalytical Chemistry 440 (1997) 125–130.
[30] S. Quillard, G. Louarn, J.P. Buisson, M. Boyer, S. Lefrant, M. Lapkowski, A. Pron, Synthetic Metals 84 (1997) 805–806.
[31] T. Lindfors, C. Kvarnström, A. Ivaska, J.of Electroanalytical Chemistry 518 (2002) 131–138.
[32] M.-C. Bernard, C. Deslouis, T. El Moustafid, A. Hugot-LeGoff, S. Joiret, B. Tribollet, Synthetic Metals 102 (1999) 1381–1382.
[33] J.E. Pereira Da Silva, S.I. Córdoba De Torresi, D.L.A. De Faria, M.L.A. Temperini, Synthetic Metals 101 (1999) 834–835.
[34] M. Baibarac, L. Mihut, I. Baltog, M. Cochet, S. Lefrant, M. Lapkowski, Synthetic Metals 96 (1998) 63–70.
[35] A. Malinauskas, M. Bron, R. Holze, Synthetic Metals 92 (1998) 127–137.
[36] C. Barbero, M.C. Miras, O. Haas, R. Kotz, J. Electroanal. Chem 310 (1991) 437–443.
[37] G.A. Planes, M.C. Miras, C. Barbero, Polym Intl. 51 (2002) 429–432.
[38] K. Chiba, T. Ohsaka, N. Oyama, J. Electroanal. Chem 217 (1987) 239–245.
[39] J. Yano, M. Kokura, K. Ogura, J. Appl. Electrochem 24 (1994) 1164.
[40] N. Comisso, S. Daolio, G. Mengoli, R. Salmaso, S. Zecchin, G. Zotti, J. Electroanal. Chem 255 (1988) 97–103.
[41] G. D'Aprano, M. Leclerc, G. Zotti, Macromolecules 25 (1992) 2145–2152.
[42] A.G. MacDiarmid, A.J. Epstein, Discuss, Faraday Soc. 88 (1989) 317–324.
[43] P.A. Kilmartin, G.A. Wright, Synthetic Metals 104 (1999) 145–156.
[44] A. Malinauskas, R. Holze, Electrochimica Acta 44 (1999) 2613–2623.
[45] A. Malinauskas, R. Holze, Ber. Bunsenges. Phys. Chem. 101 (1997) 1859–1864.
[46] R. Mažeikienė, G. Niaura, A. Malinauskas, Spectrochimica Acta Part A: Molecular and Biomolecular Spectroscopy 106 (2013) 34–40.
[47] A. Malinausakas, R. Holze, Electrochim. Acta 44 (1999) 2613-2623, and refs therein.
[48] I. Stassen, G. Hambitzer, J. Electroanal. Chem. 440 (1997) 219–228.
[49] Ref, pp 331.
[50] L.D. Claxton, T.J. Hughes, T.K. Chung, Food and Chemical Toxicology 39 (2001) 1253–1261.
[51] E.M. Geniès, A. Boyle, M. Lapkowski, C. Tsintavis, Synthetic Metals 36 (1990) 139–182.
[52] L. Duic, M. Kralic, S. Grigic, J. Polym. Sci. Part A. Polym. Chem. 42 (2004) 1599.
[53] R. Nyffenegger, C. Gerber, H. Siegenthaler, Synthetic Metals 55 (1993) 402–407.
[54] H. Tang, A. Kitani, S. Maitani, H. Munemura, M. Shiotani, Electrochim. Acta 40 (1995) 849–857.
[55] (a) C. Mailhe-Randolph, J. Desilvestro, J Electroanal Chem,262((1989) 289–295; (b) C.-H. Yang, T.C. Wen, J Electrochem Soc 144 (1997) 2078–2085.
[56] G. Zotti, S. Cattarin, N. Comisso, J. Electroanal. Chem. 235 (1987) 259–265.
[57] G.A. Planes, J.L. Rodriguez, M.C. Miras, G. Garcia, E. Pastor, C.A. Barbero, Phys. Chem. Chem. Phys. 12 (2010) 10584–10593.
[58] L. Li, H. Qiu, H. Qian, B. Hao, X. Liang, J. Phys. Chem. C 114 (2010) 6712–6717.
[59] (a) D. Wei, A. Petr, C. Kvarnström, L. Dunsch, A. Ivaska, J. Phys. Chem. C 111 (2007) 16571–16576;
(b) G.-L. Yuan, N. Kuramoto, Macromolecules 36 (2003) 7939–7945.
[60] (a) L.-H. Ai, X.-B. Wang, Z.-L. Chen, J. Jiang, Journal of Macromolecular Science, Part B 49 (2010) 953–959;
(b) J. Yano, K. Sanada, R.Y. Ooyama, K. Yousuke, K. Komaguchi, Y. Harima, Mat. Chem. Phys. 106 (2007) 279–285.
[61] M.V. Kulkarni, A.K. Viswanath, P.K. Khanna, Journal of Applied Polymer Science 99 (2006) 812–820.
[62] K. Brazdžiuvienė, I. Jurevičiūtė, A. Malinauskas, Electrochim. Acta 53 (2007) 785–791.
[63] M. Blomquist, T. Lindfors, L. Vähäsalo, A. Pivrikas, A. Ivaska, Synth. Met. 156 (2006) 549–557.
[64] M.V. Kulkarni, A.K. Viswanath, P.K. Khanna, J. Appl. Polym. Sci. 99 (2006) 812–820.
[65] K. Brazdžiuvienė, I. Jurevičiūtė, A. Malinauskas, Electrochim. Acta 53 (2007) 785–791.
[66] M. Blomquist, T. Lindfors, L. Vähäsalo, A. Pivrikas, A. Ivaska, Synth. Met. 156 (2006) 549–557.
[67] T. Iwasita, F.C. Nart, Prog. Surf. Sci. 55 (1997) 271–283.
[68] L. Dunsch, J. Electroanal. Chem 61 (1975) 61.
[69] S.-Y. Hong, Y.M. Jung, S.B. Kim, J. Phys. Chem. B 109 (2005) 3844–3850, S.-M.
[70] Barbero Cesar, J. Juana, Silber, Leonides Sereno, J. Electroanal. Chem. 263 (1989) 333–352.
[71] V. Mazine, J. Heinze, J. Phys. Chem. A 108 (2004) 230–235.
[72] L.R. Sharma, A.K. Manchada, G. Singh, R.S. Verma, Electrochimica Acta 27 (1982) 223–233.
[73] M.F. Erben, C.O. Della Védova, R.M. Romano, R. Boese, H. Oberhammer, H. Willner, O. Sala, Inorg. Chem 41 (2002) 1064–1071.
[74] C. Hartnig, J. Grimminger, E. Spohr, Electrochimica Acta 52 (2007) 2236–2243.
[75] G. Robert, D.R. Greenler, Snider, R.S. Donald Witt, Sorbello, Surface Science 11 (1982) 415–428.
[76] E.T. Seo, R.F. Nelson, J.M. Fritsch, L.S. Marcoux, D.W. Leedy, R.N. Adams, J. Am. Chem. Soc. 88 (1966) 3498.
[77] L. Duic, Z. Mandil, S. Kovac, Electrochim. Acta 40 (2013) 1681, 1195.
[78] C. Barbero, M.C. Miras, B. Schnyder, O. Haas, R. Kötz, J. Mater. Chem 4 (1994) 1775–1783.
[79] A. Watanabe, K. Mori, A. Iwabuchi, Y. Iwasaki, Y. Nakamura, O. Ito, Macromolec 22 (1989) 3521–3525.
[80] R. Mažeikienė, G. Niaura, A. Malinauskas, Polym. Degrad. & Stab. 93 (2008) 1742–1746.
[81] G.M. Morales, H.J. Salavagione, D.E. Grumelli, M.C. Miras, C.A. Barbero, Polymer 47 (2006) 8272–8280.
[82] K. Nehru, Y. Jang, S. Oh, F. Dallemer, W. Nam, J. Kim, Inorg, Chim. Acta 361 (2008) 2557–2561.
[83] D.F. Acevedo, H.J. Salavagione, A.F. Lasagni, E. Morallon, F. Mucklich, C. Barbero, ACS Appl. Mater. Interfaces 1 (2009) 549–551.